Desalination 430 (2018) 24–32

Contents lists available at ScienceDirect

Desalination

journal homepage: www.elsevier.com/locate/desal

Sand filters scaling by calcium carbonate precipitation during groundwater reverse osmosis desalination

Khaled Touati[a,*], Elbez Alia[b], Houda Zendah[a], Hamza Elfil[a], Ahmed Hannachi[b]

[a] Laboratory of Natural Water Treatment, Water Researches and Technologies Center, B.P. 273, Soliman 8020, Tunisia
[b] National Engineering School of Gabes, Omar Ibnelkhattab Street, 6029 Zrig, Gabes, Tunisia

ARTICLE INFO

Keywords:
Scaling
Sand filters
Calcium carbonate
Secondary nucleation
Super-saturation

ABSTRACT

To face water scarcity in the south, Tunisia is relying on the use of fossil water from wells as feed water in reverse osmosis desalination. This geothermal water reaches the surface with specific characteristics (50 °C < T < 70 °C, hardness ≥ 10 mM, $P_{CO2} \approx 5.10^{-2}$ atm, salinity ≥ 3 g/L). During the cooling stage, an extensive scaling takes place in the cooling towers following the release of CO_2. This phenomenon continues even in the piping system. The scaling reached the sand filter in the pre-treatment process. In the current work, the scaling in sand filters was investigated. Firstly, the nature of scaling was identified. X-Ray Diffraction (DRX) of the sand samples revealed the existence of significant quantities of aragonite form of calcium carbonate ($CaCO_3$). DRX and scanning electron microscopy (SEM) analysis revealed the presence of aragonite crystals in the raw water. Investigations showed that these crystals trapped in the sand filter act as seeds inducing secondary nucleation of $CaCO_3$. The study showed that the raw water is over saturated with respect to both calcite and aragonite, while it is under saturated relative to the $CaCO_3$ monohydrate form. It was suggested that the feed water is at meta-stable state, and crystal nucleation can only be driven through seeding. Laboratory experiments using the raw water with simulated sand filter confirmed the inevitable secondary nucleation supported by aragonite crystals. Consequently, the suggested solution was a water acidification ahead of the sand filtration operation instead of past of it in the desalination process.

1. Introduction

Water is an indispensable resource for life. This essential source is widely used in several fields such as agriculture, industry and domestic needs. In nature, there are four main sources of raw water; rainwater, surface waters, subterranean waters and seawater [1]. All these categories revealed different qualities made up of the different salts naturally dissolved [2,3]. Nowadays, the world is facing the problem of water scarcity [4,5]. To meet the increase of water demand and limited supply of drinkable water, the need for alternative fresh water sources is strongly required. Desalination is one of the most useful processes that provides alternative and sustainable solution for water scarcity problems [6,7]. Water desalination techniques, especially based on membrane separation, are in full expansion in the world. Like many Mediterranean countries, Tunisia has installed several reverse osmosis (RO) desalination plants. In literature, most studied problems in desalination process are mainly related to membrane fouling and scaling [8–12]. This is axiomatic due to the fact that the membrane is the key piece in separation process. Consequently, intense researches were made to provide an adequate pretreatment to minimize the risk of fouling and salt depositions that reduce the lifetime and membrane performance [13–15]. However, in our best knowledge, fouling and scaling in filters are considerably neglected. Filters guarantee the well-functioning of the process. Therefore, filters performance also should be optimized. In the southern of Tunisia (RO desalination plant, Chott El-Fejjej- Gabes district), the treated raw water is essentially groundwater. Fossil water from boreholes whose depths vary between 1000 and 3000 m are exploited [16]. The water temperature at the outlet of boreholes varies between 50 and 70 °C, its calcium concentration and alkalinity are of the order of 10 and 2 mM, respectively, the salinity is > 3 g/L and the dissolved carbon dioxide CO_2 is relatively high ($P_{CO2} \approx 5.10^{-2}$ atm) [16]. Drilling rates vary from 45 to 140 L/s [17]. Chott El-Fejjej desalination plant has a series of sand filters which suffer from the increase of sand filtering mass due to the accumulation of inorganic deposit that adheres to the sand grains. This problem requires slow and expensive regeneration. During the cooling step, which is a fundamental operation before water use, a gigantic quantity of scale is deposited following the escapement of CO_2. The deposition continues in

* Corresponding author.
E-mail addresses: kha.touati@gmail.com (K. Touati), ahmed.hannachi@enig.rnu.tn (A. Hannachi).

https://doi.org/10.1016/j.desal.2017.12.037
Received 19 September 2017; Received in revised form 6 December 2017; Accepted 19 December 2017

the pipes and causes a severe problem to the exploitation of this water. The decarbonation of the Chott El-Fejjej water would have the advantage of avoiding deposits of scale in the cooling towers and in the sand filters, reducing the hardness of the raw water and the recovery rate of the desalination plant. In this situation, the conventional solution is to decarbonate with lime. However, besides the large and expensive consumption of such reagent, which is not readily available in the Gabes desert, this process generates large amounts of carbonated sludge. Thus, if this treatment is considered, it supposes a complex apparatus using a fluidized bed crystallization support [18] whose good functioning may be compromised with the presence of large amounts of magnesium [18]. In this work, an alternative solution was suggested. The technical intervention consists of avoiding the nucleation of calcium carbonate in the raw water. For that, the raw water was, firstly, characterized with "calco-carbonic equilibrium" point of view. Secondly, the increase of sand filter mass was estimated experimentally. Thirdly, the sand filter was simulated in lab-scale for testing synthetic and real water. The filter was designed to operate continuously and experimental conditions were very close to reality, since Chott El-Fejjej's refrigerants are using air ventilation, which would facilitate the adaptation on an industrial scale. Finally, the increase of the sand filter mass was assessed to prove that the secondary nucleation of calcium carbonate is inevitable. Consequently, the most suitable solution to optimize the performance of the sand filters was taken according to experimental results.

2. Meta-stability in calco-carbonic system

In the calco-carbonic system, hydrated forms play an important role in the process of calcium carbonate nucleation [25]. In fact, spontaneous nucleation, called primary, can only take place if one of the hydrated forms, called precursor, appears. If the calco-carbonic solution is supersaturated with respect to the amorphous calcium carbonate form (ACC) (see Zone A1 – Fig. 1), ACC variety plays the role of a precursor for a homogeneous and instantaneous nucleation, regardless the nature of the walls and foreign particles [19,20]. In the case where the product of the ionic activity of the solution is between the solubility product of the ACC and that of the calcium carbonate monohydrated (CCM) (Zone A2 - Fig. 1), heterogeneous primary nucleation takes place, the precursor here is the monohydrate form. This nucleation depends strongly on the nature of the walls and foreign particles, especially for low saturation solutions with respect to the monohydrate form. If the state of super-saturation does not result in the formation of one of these precursors (CCM and ACC), the system remains in a state of meta-stability. In other words, a super-saturation of the calco-carbonic system with respect to the anhydrous forms is insufficient for a spontaneous nucleation of the $CaCO_3$. The meta-stability zone of the

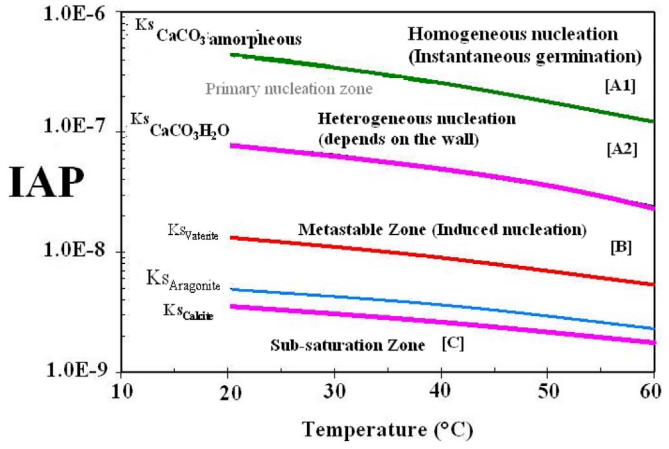

Fig. 1. Meta-stability diagram of calco-carbonic system.

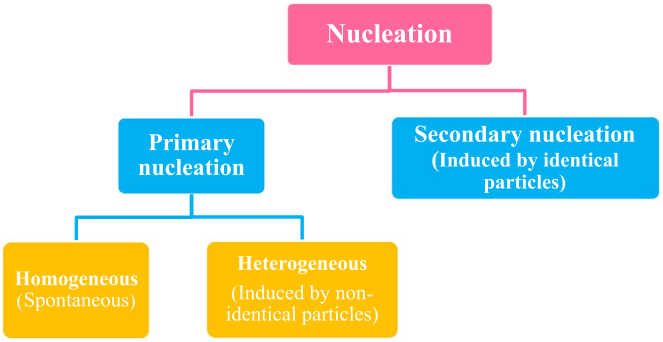

Fig. 2. Schematic of nucleation mechanisms.

calco-carbonic system has been delimited thermodynamically [21], it lies between the calcite solubility product and CCM solubility product (Zone B – Fig. 1). This meta-stability can be broken by seeding with $CaCO_3$ crystals. Therefore, a secondary nucleation supported by seed crystals of $CaCO_3$ occurs.

2.1. Mechanism of nucleation

Nucleation is a process in which the free or dissolved ions or molecules gather and organize to form the so-called germ. The appearance of the crystals can only be achieved when a degree of super-saturation is reached. Three stages can be distinguished during the precipitation of calcium carbonate: nucleation, dehydration and crystal growth. The process begins with the ions that agglomerate forming a "cluster". The grouping of these aggregates forms a colloidal nucleus which grows and gives a stable crystal. Primary nucleation and secondary nucleation are distinguished (Fig. 2). A) Homogeneous nucleation: It is obtained when the nucleus develops only in the liquid phase and is not influenced by the presence of impurities in the reaction medium. The number of molecules in a stable germ can vary from about 100 to several thousand. The actual formation of such a nucleus results from the simultaneous collision of the number of necessary molecules. This is a highly unlikely phenomenon. The process of forming such a germ involves a certain energy called the free energy of activation of nucleation. B) Heterogeneous nucleation: Nucleation is said to be heterogeneous when the nucleus develops on a support or in the presence of impurities. These impurities can act as an accelerator as well as an inhibitor [24]. It is generally appropriate that heterogeneous nucleation can be initiated to a lower degree of super-saturation than homogeneous nucleation. The variation in free enthalpy associated with heterogeneous nucleation is lower than that associated with homogeneous nucleation [21,24]. The secondary nucleation, in a weakly supersaturated solution, is induced and supported by seed crystals of the same nature as the precipitate. In this type of nucleation, the affinity between the crystals of the solute formed and the seed crystals (solid surface) is total, which corresponds to a critical energy of zero nucleation [21,24].

3. Materials and methods

3.1. Sand filter description and problematic

The separation is carried out by means of a static filter bed. The filter should be made by chemically insoluble material which is inert with respect to aggressive water and capable of undergoing the intense friction caused by the sand washes without crumbling. A conventional filter is presented in Fig. 3. It consists of: *i*) a filter bed made of sand and anthracite, *ii*) a gravel support, *iii*) a filter background, *vi*) a device for washing the sand bed, *v*) a washing water discharge chutes, and *iv*) valves for water inlet and outlet as well as control devices for the various phases of the operation.

The filter feed is provided by overflowing the water from the middle

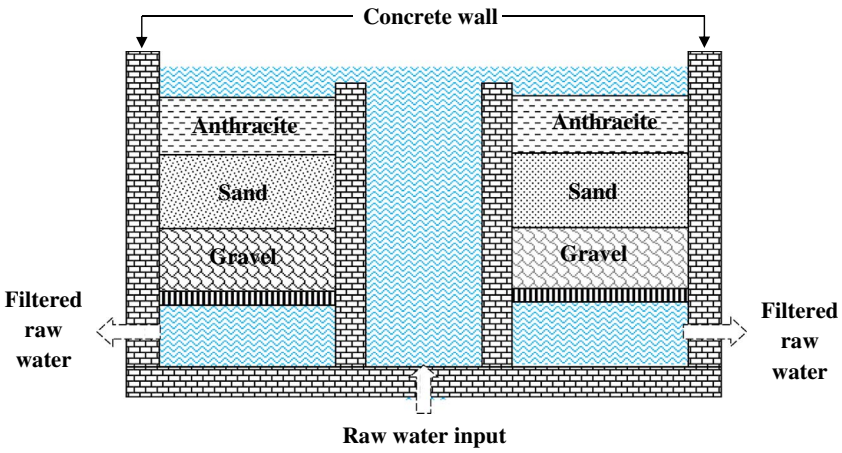

Fig. 3. Schematic of the sand filter used in groundwater desalination plant (Gabes, Tunisia). The desalination plant has 8 identical concrete sand filters, approximately 9 m long and 6 m wide. The water circulation in the filters is done from top to bottom. The sand filter consists essentially of: Filter bottom: this is the structure that separates the filter medium from the filtered water. It is equipped with nozzles that allow the collection and removal of filtered water and a uniform distribution of the washing water. Filter medium consisting of 3 layers of gravel, sand and anthracite with grain sizes of 2–5, 0.4–0.8 and 0.8–1.6 respectively.

column. The filter removes all particles with diameter superior to 45 μm. During their inevitably winding path, the particles in suspension strike those of the bed and cling to them gradually. The retention of the particles will be done by simple sieving effect in the upper part of the filter for the large particles, and by the effect of the wall at different levels inside the filter for the finest particles. Thus, the filtration efficiency of the filter will be greater than the grain diameter, then, the residence time of the particle in the filter will be longer. It is therefore understood that the choice of parameters such as the particle size of the filtering media, the height of the layer and the filtration rate play a fundamental role on the efficiency of the process [16].

In recent years, a phenomenon of cake formation on filter bed has been observed. It has been found that the fouling in sand filter results from an accumulation of deposition in the filter material [16]. The problem of scaling resulting from an accumulation of deposition in the filtering mass; which leads to the mass increase of the filter medium. The phenomenon of cake formation takes place every six months. In the following photographs (Fig. 4), relatively large aggregates are seen floating on the filter bed and clearly showing the bulk of the filter material. The agglomerates thus formed reduce the cross-section of the water through the filter medium and reduce the efficiency of the treatment. It is therefore important to seek to optimize their performance in order to improve the quality of the filtered water and increase the filtration cycle time before regeneration.

The sand filters of the Gabes desalination plant retain suspended solids and subsequently reduce the Silt (Silt density index) from 4 to about one unit [16,17]. A washing of the filtering mass takes place against the current with air and water, whenever the pressure drop at the sand filter reaches the permissible threshold. The water from the desalination plant (and the sand filter) is a mixture of water from several boreholes, which allows changes in several physicochemical characteristics of the raw water. Therefore, the Upper and lower limits of physical-chemical characteristics of raw water were determined Table 2. Full chemical analysis of the raw water is presented in Table 1. Two predominant salts which are likely to precipitate are calcium carbonate and gypsum ($CaSO_4{\cdot}2H_2O$). Estimation of ionic activity coefficient was useful to determine the two salts precipitation and super-saturation. Pitzer simplified model was used to calculate all the activity coefficients [22]. Super-saturation Ω is defined as the ratio of the ionic activity product (IAP) and the solubility product (K_s): Their super-saturation can be calculated using the following two formulas [23]:

$$\Omega_{/gypsum} = \frac{a_{Ca^{2+}} \times a_{SO_4^{2-}}}{K_{s/gypsum}} = \frac{\gamma_{Ca^{2+}}[Ca^{2+}] \times \gamma_{SO_4^{2-}}[SO_4^{2-}]}{K_{s/gypsum}} \quad (1)$$

$$\Omega_{/CaCO_3} = \frac{a_{Ca^{2+}} \times a_{CO_3^{2-}}}{K_{s/CaCO_3}} = \frac{\gamma_{Ca^{2+}}[Ca^{2+}] \times \gamma_{CO_3^{2-}}[CO_3^{2-}]}{K_{s/CaCO_3}} \quad (2)$$

3.2. Estimation and characterization of sand filter mass increase

3.2.1. Strategy

To estimate the filter mass increase, the calcium carbonate from a sample is dissolved by two methods: dissolution by bubbling of carbon dioxide, and treatment of the sample using a strong acid. Then, the calcium hydrotimetric (TCa) and alkalinity (TAC) are determined experimentally in the obtained solutions. The first series of using CO_2 bubbling are described in the Supplementary Contents. In a second series of experiments, the starting solution is attacked by concentrated sulfuric acid (90% w/w), which rapidly dissolve the calcium carbonate

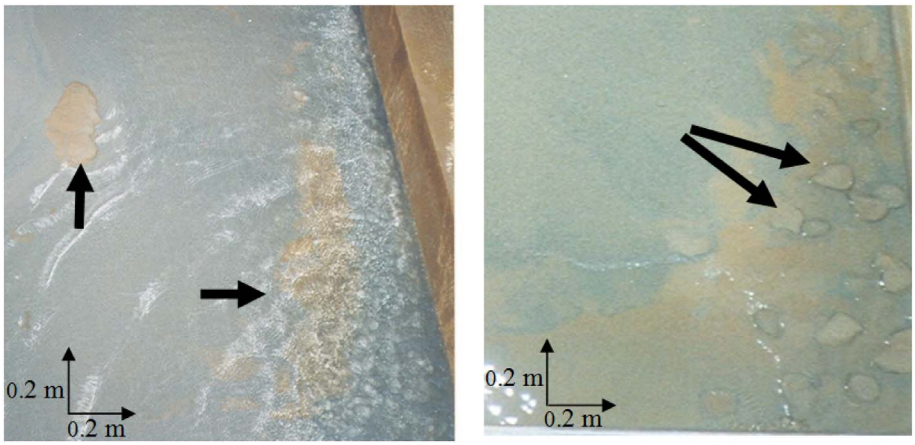

Fig. 4. Photos showing the presence of agglomerates on the surface of the sand filter.

Table 1
Upper and lower limits for some physical-chemical characteristics of raw water.

	TDS mg/L	pH	T(°C)	Turbidity NTU	Ca^{2+} mg/mL	Mg^{2+} mg/mL	HCO_3 mg/mL	SO_4^{2-} mg/mL	Na^+ mg/mL	Cl^- mg/mL
Min	3000	7.4	25	0.3	340	45	98	1100	480	800
Max	3200	8.0	35	0.9	400	110	120	1200	510	830

Table 2
Chemical analysis of the raw water is given in.

Cations		Anions	
entity	Concentration (mg/L)	entity	Concentration (mg/L)
Ca^{2+}	388	HCO_3^-	128
Mg^{2+}	75	Cl^-	820
Na^+	500	SO_4^{2-}	1172
K^+	48	NO_3^-	< 0.2
NH_4^+	0.2	NO_2^-	< 0.02
Fe^{2+}	0.2	F^-	0.3
Al^{3+}	0.72	PO_4^{3-}	< 0.1
		SiO_2	35
TDS (g)		3.160	
pH		7.6	

Table 3
Quantity of dissolved $CaCO_3$.

		Initial mass (g)	Final mass (g)	Total dissolved mass (g/Kg of sample)	$CaCO_3$ (g/Kg of sample)	Mass ratio (%)
Carbonic	1st	200	197.3	13.6	10.8	80
Acid test	2nd	50	49.2	15.2	13.8	91
Sulfuric acide test		50	47.3	54.8	54.2	> 98

Table 4
Raw water characteristics.

Salinity	pH	T (°C)	TCa (°f)	TAC (°f)	$\Omega_{/CaCO3\cdot H2O}$	$\Omega_{/Aragonite}$
3.2	7.9	27.2	93	9	0.4	6.1

Table 5
Characteristics of the treated solution.

pH	TCa = TAC (°f)	$\Omega/_{aragonite}$	$\Omega/_{CCM}$
7.8	25	5.83	0.39
8.0	25	9.24	0.62
7.92	25	7.10	0.47
7.91	30	10.0	0.67
7.90	35	13.3	0.89

present in the filter material. The chemical reaction describing the acid attack is as follows:

$$H_2SO_4 + CaCO_3 \rightarrow Ca^{2+} + SO_4^{2-} + H_2O + CO_2(g) \quad (3)$$

An increase in TCa was noticeably observed. At the end of the experiment, the solutions are filtered and dried. Thus, the solid recovered was analyzed by Infra-Red spectroscopy (IR).

3.2.2. Sand filter simulation

To realize experimental tests on synthetic and real solutions, a laboratory sand filter, presented in Fig. 5, was built to simulate the one used in RO desalination plant. The sand filter made of Plexiglas consists of: *i*) a sand bed made of sand grains. The average size was between 0.6 and 1 mm forming a thickness of 10.5 cm, *ii*) a gravel bed with average size 2.4 mm forming a porous layer with a height of 3.2 cm, *iii*) a floor that supports the entire filter medium. The type of filter designed is a fast sand filter. To guarantee homogeneous experimental conditions, the medium used to fabricate the sand filter (sand, gravel…etc) presented the same characteristics of the one used in RO plant. The water sample passes under a constant hydraulic load through the filter bed. The flow takes place by gravity from top to bottom. The filtration rate, v, is calculated by the following equation:

$$v = \frac{Q}{S} \quad (4)$$

where Q is the feed water flow, and S is the section of the filtration column.

3.2.3. Granulometry of the filtration media

The granulometric plot of the sand was established by passing over the sieve columns. The ratio of the mass passage across the sieve (⌀) is shown in Fig.6. Clearly, the effective diameter (D_E) and the coefficient of uniformity (C_U) are readily accessible. C_U represents the ratio between the diameter which allows 60% of the particles to pass and that which allows 10% to pass ($D_{60\%}//D_{10\%}$). The effective diameter corresponds to the mesh size of the sieves which allow 10% of the mass of the sample to pass. In our case, D_E = 0.49 mm and C_U = 1.7. If C_U is < 2, the grain size is considered tight and uniform. Obviously, the increase of the sieve diameter leads to the increase of the mass passage across the sieve. When the sieve diameter is superior to 0.3 mm, ⌀ increases drastically because most of the grain size is likely inferior to this value. In the opposite case, ⌀ barely increases. Consequently, the choice of the sieve diameter should be chosen around 0.3 mm.

3.2.4. Filtration cycle sequences

Once the filter material was put in place and before starting the experiment, a quantity of aragonite seed is distributed over the entire surface of the filter material. These seeds were used to provoke secondary nucleation of calcium carbonate. The experiment involves passing a supersaturated calco-carbonic solution through the sand filter equivalent to the raw water of the real desalination plant. In other words, the solution must be supersaturated with respect to aragonite without the possibility of spontaneous primary nucleation of calcium carbonate. This synthetic solution is circulated, in a closed circuit, through the filter material via a pump. The temperature of the solution is maintained at 25 °C. The pH, calcium concentration and alkalinity of this solution are monitored throughout the experiment. The pressure drop at the filter material of the sand filter is also followed by a differential pressure gauge; it gives an idea about the fouling of the sand filter. The pH of the treated solution was continuously controlled in such a way that the latter remains in meta-stability state. The calcium concentration decreases gradually until it reaches an equilibrium value, where secondary nucleation of the calcium carbonate stops. The experiment is then stopped and then taken up with a new calco-carbonic solution. During filtration operation, a substantial rise in the water level above the filter material can be detected. In this case, the feed rate is adjusted by flow-meter in such a way that the level of water is fixed along the experiment.

The pure calcium carbonate solution is prepared by bubbling CO_2 in a solution that contains pure $CaCO_3$ suspended in distilled water. This

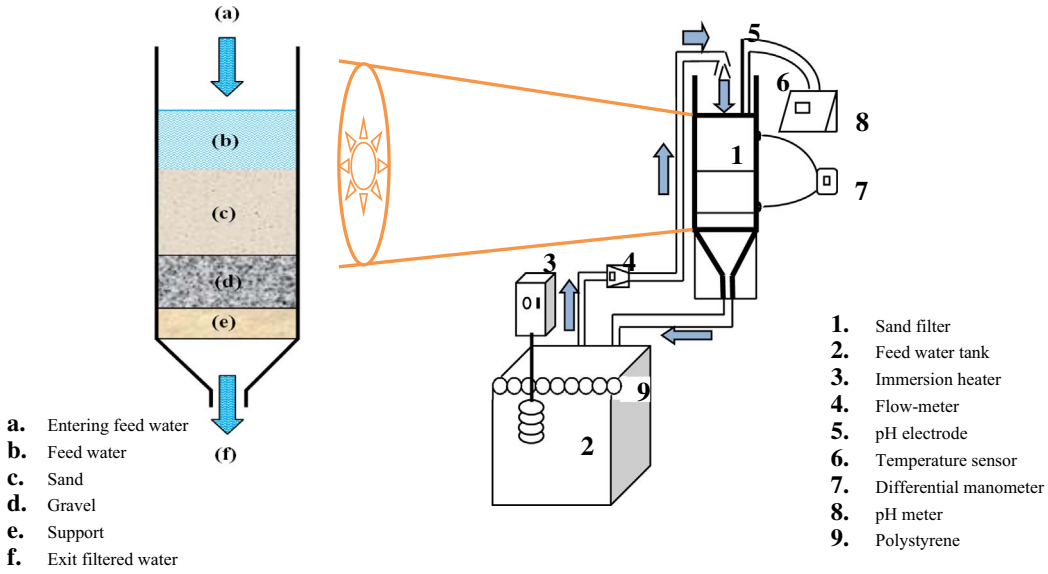

Fig. 5. Schematic of laboratory sand filter and experimental apparatus.

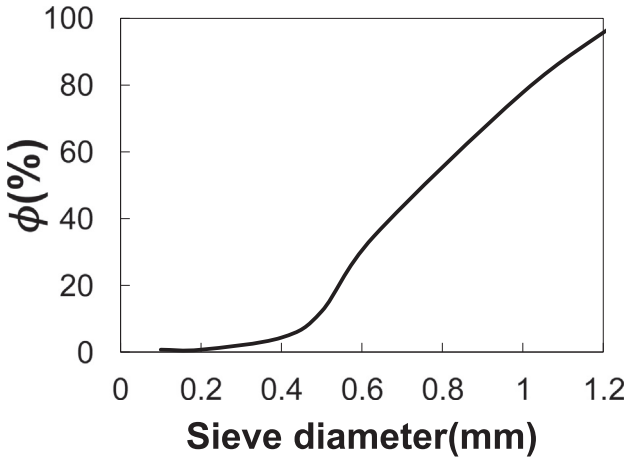

Fig. 6. Graphical presentation of sand particle size analysis.

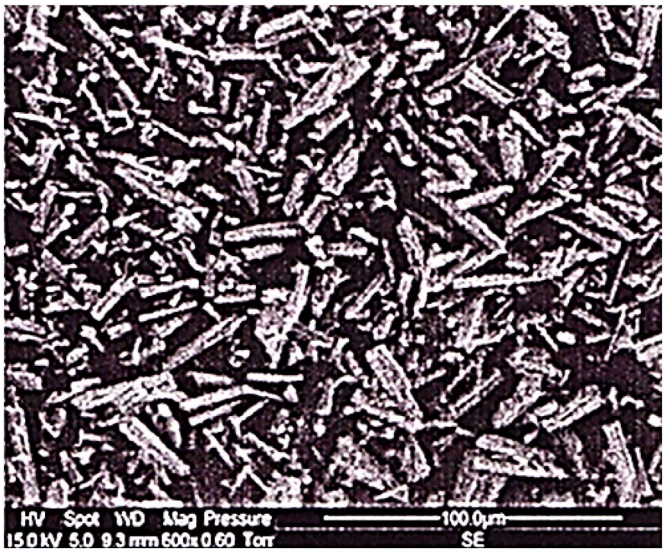

Fig. 7. Microscopic observation of crystal recovered from water pipes. The SEM revealed the presence of only one form of $CaCO_3$ (needles form).

solution is stirred under a CO_2 atmosphere for a few hours until the total dissolution of the $CaCO_3$. To obtain 1 L of a calcium carbonate solution with a calcium concentration of 25 °f, it is sufficient to dissolve a mass of 0.250 g of pure $CaCO_3$ ($M = 100.1\ g{\cdot}mol^{-1}$) in 1 L of distilled water. It should be noted that 25 °f = $25.10^{-4}\ mol{\cdot}L^{-1}$ of $CaCO_3$.

3.2.5. Aragonite seed preparation

The added seeds are aragonite particles recovered from the geothermal water pipes of Chott ElFejjej. The photos obtained by the Scanning Electron Microscopy technique show that these seed crystals consist of aragonite needles (Fig. 7). This is also confirmed by the X-ray diffraction pattern showed in Fig. 8. A mass of 2 g of seed is slightly crushed and introduced into the upper part of the sand filter during operation.

4. Results and discussions

4.1. Characterization of deposit in sand filter

In order to know the nature of precipitated deposition at the sand filters, samples of the bulk filter material were analyzed by the X-ray diffraction method. A sample of fresh sand (before use) was also analyzed. The virgin sand used as a filtration medium consists mainly of quartz (SiO_2) combined with Coesite as shown by the diffractogram presented in Fig. 9-a. The diffraction patterns of the fouled sample revealed, in addition to quartz, picks indicating the presence of calcium carbonate in the form of aragonite (see Fig.9-b). It is therefore a phenomenon of precipitation of calcium carbonate which is essentially related to the quality of the water that feeds the sand filters. Hence, it is possible to estimate the amount of tartar contained in this sample.

4.2. Estimation of the amount of precipitated $CaCO_3$

It is proposed in this section to determine the amount of precipitated calcium carbonate in the sand filter of the real desalination plant. For this, the calcium carbonate from a sample is dissolved by two methods as described in Section 3.2 and Supplementary Contents.

4.2.1. Treatment with sulfuric acid

After a three-day stay of 50 g of sand filter in a sulfuric acid solution, filtration of this solution using Büchner device was carried out. The filtrate collected had a calcium content of 221.2 °f. The alkalinity

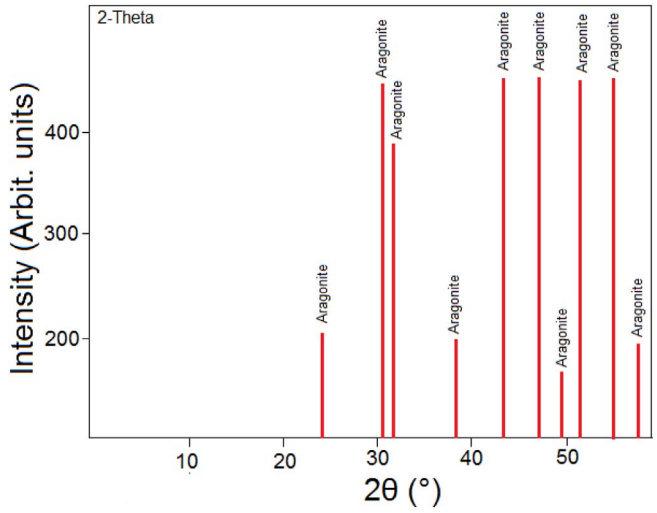

Fig. 8. X-ray diffraction diagram of crystals recovered from water pipes. The aragonite is the only form present in the crystals.

was not quantified due to the fact that its determination in an acidic solution is erroneous. This analysis allowed the estimation of the dissolved calcium carbonate mass at 54.2 g/Kg of sample assuming that all Ca^{2+} ions are in $CaCO_3$ form. The mass difference of the sample before and after treatment with acid gave a mass loss of about 54.8 g/Kg (see Table 3). The proportion of $CaCO_3$ in the dissolved fraction was 98%. Analysis of the samples (fouled, pure and treated with acid) by infrared spectrophotometer gave the spectra shown in Fig.10-b. The bands attributed to the presence of calcium carbonate (713 cm^{-1}, 874 cm^{-1} and 1423 cm^{-1}) which are in the spectrum of the fouled sample are virtually absent in that of the treated solid. Thus, the treatment using a strong acid dissolved almost the totality of calcium carbonate present in the fouled filter material. Two new bands (601.7 cm^{-1} and 660.5 cm^{-1}) appeared on the spectrum of the treated sample attributed to calcium sulfate dihydrated. In fact, the treatment of the sample containing calcium carbonate was carried out with H_2SO_4, which leads to the simultaneous existence of Ca^{2+} ions and SO_4^{2-} ions at non-negligible concentrations. Since the solubility of the gypsum does not depend on the pH of the solution, the solubility limit of the solution (~2.2 g/L) can be rapidly exceeded and leads to gypsum precipitation.

4.3. Characterization of raw water from cooling towers

A physicochemical analysis was necessary to evaluate the scaling character of the supply water of the station. The geothermal water of the region of Elhamma-Gabes arrives at the desalination plant at a temperature close to 30 °C and a pH of 8. At this level, the water is in a sub-saturation state with respect to $CaCO_3{\cdot}H_2O$ (see Table 4); therefore, no spontaneous nucleation of $CaCO_3$ can occur. However, this solution is supersaturated with respect to aragonite. So, the secondary nucleation induced by aragonite crystals may occur as shown in Fig. 11. Analysis by SEM of the suspended matter in the feed water, collected on a 0.45 µm filter, showed the presence aragonite traces (Fig. 12-a). The same shape was obtained in the cooling towers of geothermal water and pipelines (Fig. 12-b). The traces of aragonite crystals contained in the raw water are trapped in the sand filters and constitute seeds with secondary nucleation. These crystals will induce precipitation of the calcium carbonate which subsequently causes the increase of filter material mass.

4.4. Calco-carbonic meta-stability of raw water

In order to study the water scaling capacity of the desalination plant, calcium carbonate precipitation experiments were carried out. A solution of raw water is placed in a double-walled reactor at a temperature of 30 °C. During the first 10 min of the experiment, the solution is bubbled by atmospheric air to increase the pH to about 8. Thereafter, agitation is ensured by means of a magnetized stirring. A pH plateau was noticed in Fig. 13-a, and the calcium concentration did not vary for 140 min, indicating the calco-carbonic stability of the raw water. The solution is then seeded with aragonite crystals (0.1 g) finely ground. The examination of the plots describing the evolution of the TAC and the pH as a function of time (Fig. 13-a and b) revealed the existence of a phase of latency. During this phase, the values of TAC and pH stabilize for > 2 h. During this period, no possibility of spontaneous nucleation was observed. Seeding with 0.1 g of aragonite triggered the precipitation. In fact, the drop of the solution alkaliny, accompanied by a decrease in the pH, indicated the nucleation of $CaCO_3$. This nucleation is of secondary type supported on aragonite seed crystals. In order to better interpret the results of this experiment, the evolution of the Ion Activity Products (IAP) in relation to the solubility products of the various forms of the calcium carbonate is illustrated in Fig. 13-c. This figure shows that the maximum value of IAP reached is in the meta-stability zone of the calco-carbonic system [24,25], which explains the stability of this solution for > 2 h. This meta-stability has been broken (fall of IAP) by the aragonite crystals added to the solution which is supersaturated with respect to aragonite.

In sand filters, the raw water comes into contact with the sand and gravel. In order to study the calco-carbonic meta-stability of this water in contact with the components of this filtering material, the previous experiment was repeated with double seeding with sand and gravel in two different times. The solution had maintained its meta-stability for more than 10 h as shown in Fig. 13-b. No precipitation of calcium carbonate was observed. In addition, the filter material was inert with

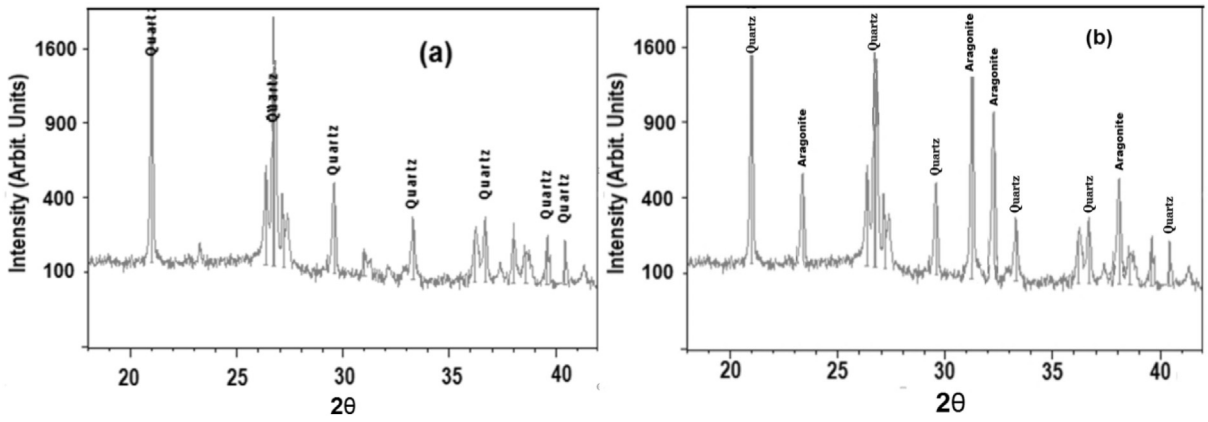

Fig. 9. DRX diagram of virgin sample of sand filter (a), and a sand filter sample with deposit (b).

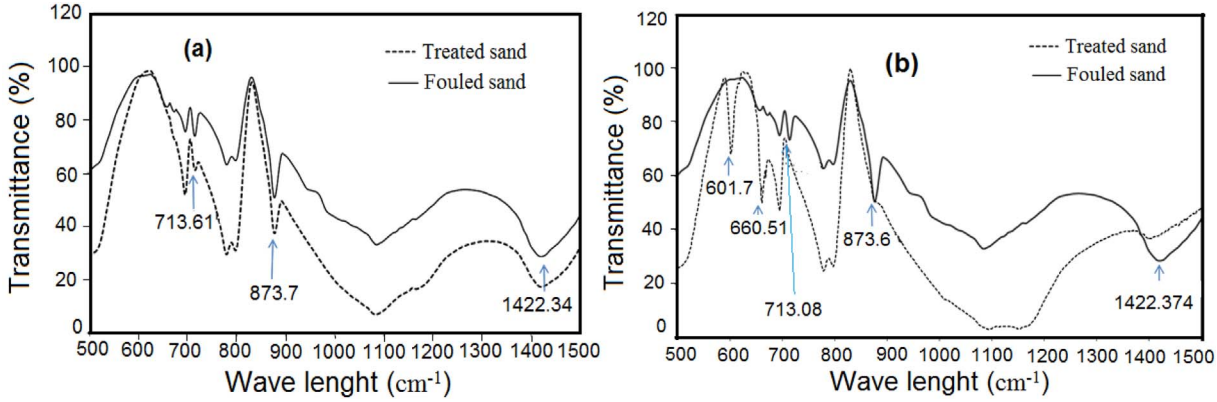

Fig. 10. IR Spectrums of treated and fouled samples of sand. (a): IR Spectrum results for sand treated with carbonic acid. (b): IR Spectrum results for sand treated with sulfuric acid.

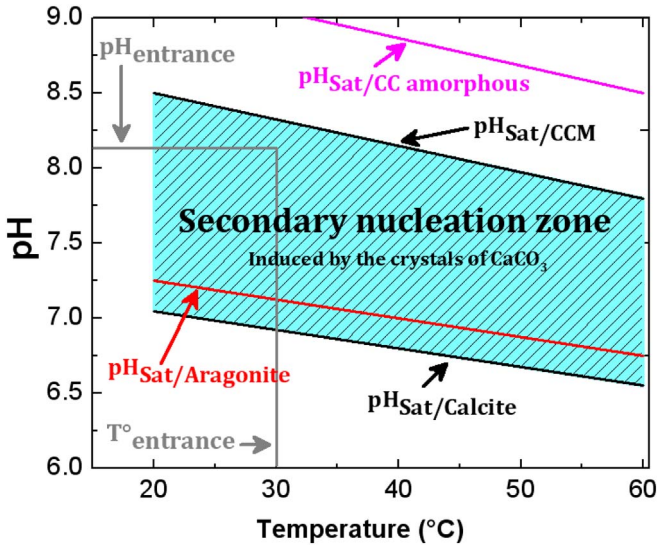

Fig. 11. Positioning of the feed water with respect to the saturation pH of the various $CaCO_3$ forms.

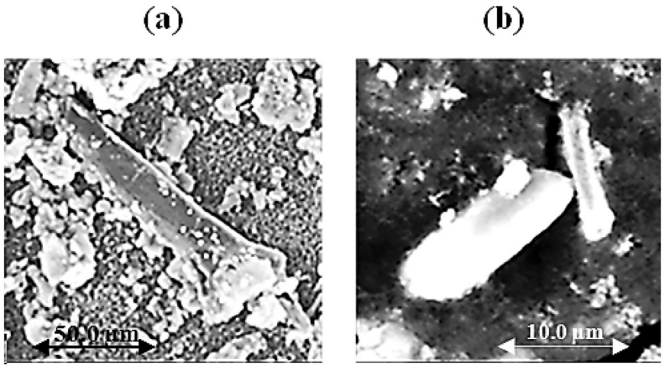

Fig. 12. Microscopic observations of suspended matter deposition in raw water. (a) Sample collected from filtering raw water using 0.45 µm filter. (b) Sample collected from cooling towers.

respect to the calco-carbonic stability of the water. It can be concluded that the water supply to the desalination plant disclose a calco-carbonic meta-stability which can only be broken by the presence of calcium carbonate crystals. These types of crystals transported, in very small quantities, by water mostly coming from cooling towers are stopped and trapped in the sand filter volume. They constitute seeds to support secondary nucleation of $CaCO_3$ which subsequently causes the mass increase in sand after a few months of operation. The filter material was inert with respect to the calco-carbonic stability of the water.

4.5. Simulation of the increase of sand filter mass

In order to study the simulation of the sand filter mass, a series of experiments were carried out in a closed circuit. The laboratory sand filter, presented previously in Fig. 5, was traversed by a meta-stable calco-carbonic solution. In a given experiment, the flow rate is fixed and the change in calcium concentration, pH and ΔP is noted. The objective is to have only a secondary nucleation of the calcium carbonate induced by the seeds of aragonite during the passage of the water through the filtering mass of the sand filter. Thus, the solution tested should be a meta-stable calco-carbonic solution where any risk of primary nucleation (spontaneous precipitation) is zero. A meta-stable calco-carbonic solution means that it is saturated with respect to the calcium carbonate monohydrate ($\Omega_{/CCM} < 1$) [24]. A secondary nucleation induced by aragonite crystals means that its super-saturation with respect to aragonite is > 1 ($\Omega_{Aragonite} > 1$). The chosen solution should therefore have the following characteristics at working temperature (30 °C.): $\Omega_{/CCM} < 1$ and $\Omega_{Aragonite} > 1$. The characteristics of the treated solution are summarized in Table 5. As seen in Fig. 14, for 13 h, the calco-carbonic solution containing no aragonite crystals passes through the sand filter at a rate of 2.5×10^{-2} L/min with no change in the calcium concentration. In fact, the solution treated is at a pH of the order of 8 to 8.2 is always under saturated with respect to the $CaCO_3{\cdot}H_2O$ ($\Omega_{/CCM} < 1$). Thus, spontaneous precipitation has no chance of occurring. After a period of about 12 h and a half, 2 g of aragonite seeds are placed on the surface of the filter material. About 15 min later, the fall in calcium concentration begins to be noticeable. In fact, the added aragonite crystals are trapped in the sand filter and constitute seeds with secondary nucleation. These crystals played the role of a trigger for the phenomenon of secondary precipitation of calcium carbonate in the sand filters. Nucleation is supported by aragonite crystals. After 40 h of operation, the calcium titer of the solution stabilizes at a value of the order of 14 °f, indicating the end of precipitation of the calcium carbonate, which represents the kinetic equilibrium under these experimental conditions.

5. Conclusion

In the current work, scaling by calcium carbonate precipitation in sand filter during ground water desalination was investigated. For that, a RO desalination plant located in the south of Tunisia, suffering from sand filter scaling, was studied. During diagnosis of the plant, it was found that the raw water has also led to scaling problems in the atmospheric refrigerants and water pipes. This problem was aggravated by the existence of agglomerate that prevents the filter from operating properly. The diagnosis of the sand filters, experiments and tests carried out during this work showed that scaling was caused by the crystals of

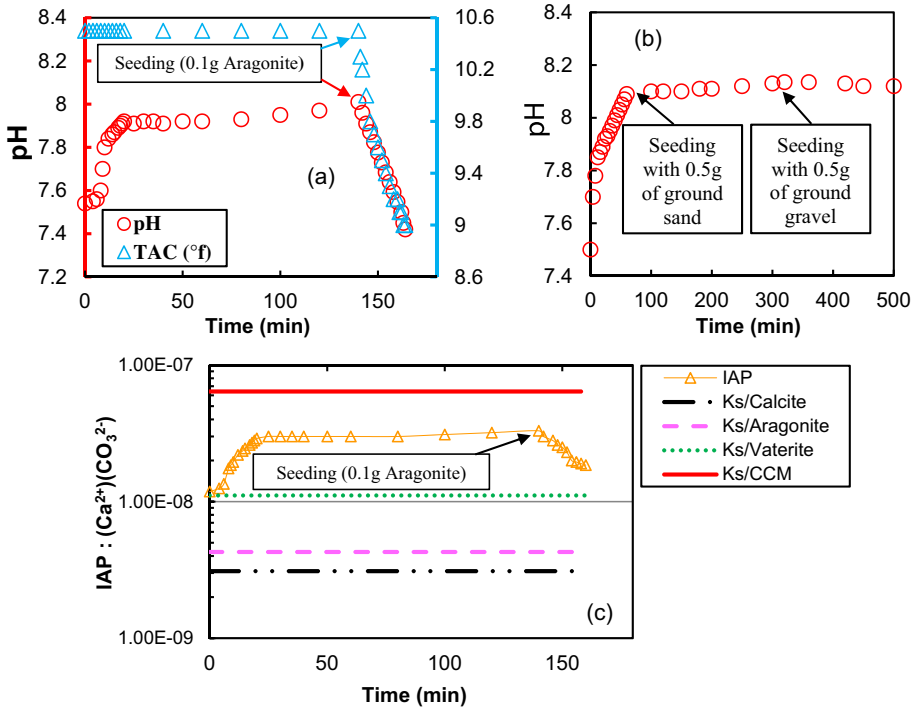

Fig. 13. Calco-carbonic meta-stability for the raw water. (a): Releasing the meta-stability of the feed water of by seeding with 0.1 g Aragonite. (b): Double seeding of raw water with sand and gravel. (c): Evolution of IAP as function of time.

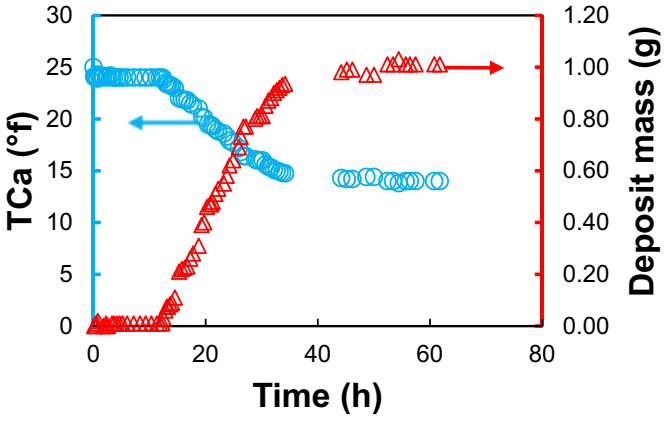

Fig. 14. Variation of the calcium hydrotimetric and deposit mass in the sand filter as function of operation time.

aragonite which are transported from the cooling towers to the desalination station. These crystals, which are trapped in the sand filters and covered by the cooled geothermal water, led to secondary nucleation. Consequently, calcium carbonate precipitated, which led to an increase of the filter medium mass. This mass increase caused a loss of charge that will aggravate with time. Then, the inhibition of the aragonite crystals formation, the trigger of the secondary nucleation, is primordial. The solution proposed to solve this problem is to realize an acidification of the water upstream of the filter to ensure that the crystals of aragonite no longer persist.

Nomenclature

C_U	coefficient of uniformity. (−)
D_E	effective diameter of sand particle. (mm)
IAP	ionic activity product. (−)
K_s	solubility constant of calcium carbonate. (−)
K_w	constant of the water dissociation. (−)
K_1	constant of the first dissociation of carbonic acid. (−)
K_2	constant of the second dissociation of carbonic acid. (−)
m_e	mass of sand filter sample. (g)
TAC	alkalinity. (g/L)
TCa	calcium hydrotimetric. (g/L)
TDS	total dissolved salts. (g/L)
Q	feed water flow. (m^3/s)
S	section of the filtration column. (m)
v	filtration rate. (m/s)
V_e	volume of tested water. (L)
$\Omega_{/gypsum}$	super-saturation of the solution regarding the gypsum. (−)
$\Omega_{/CaCO_3}$	super-saturation of the solution regarding the calcium carbonate. (−)
$\Omega_{Aragonite}$	super-saturation of the solution regarding the aragonite. (−)
$\Omega_{/CCM}$	super-saturation of the solution regarding the calcium carbonate monohydrated. (−)
ΔP	applied pressure. (bar)

Appendix A. Supplementary data

Supplementary data to this article can be found online at https://doi.org/10.1016/j.desal.2017.12.037.

References

[1] Cejna Anna Quist-Jensen, Francesca Macedonio, Enrico Drioli, Membrane technology for water production in agriculture: desalination and wastewater reuse, Desalination 364 (2015) 17–32.
[2] Fan Zhu, Chemical composition, health effects, and uses of water caltrop, Trends Food Sci. Technol. 49 (2016) 136–145.
[3] The influence of temperature and seawater composition on calcite crystal growth mechanisms and kinetics: implications for Mg incorporation in calcite lattice, Geochim. Cosmochim. Acta 73 (2) (2009) 337–347.
[4] Maria Christina Fragkou, Jamie McEvoy, Trust matters: why augmenting water supplies via desalination may not overcome perceptual water scarcity, Desalination 397 (2016) 1–8.
[5] Tiziano Distefano, Scott Kelly, Are we in deep water? Water scarcity and its limits to economic growth, Ecol. Econ. 142 (2017) 130–147.
[6] Shiva Gorjian, Barat Ghobadian, Solar desalination: a sustainable solution to water crisis in Iran, Renew. Sust. Energ. Rev. 48 (2015) 571–584.
[7] Renewable energy integrated desalination: A sustainable solution to overcome future fresh-water scarcity in India, Renew. Sust. Energ. Rev. 73 (2017) 594–609.
[8] P.S. Goh, W.J. Lau, M.H.D. Othman, A.F. Ismail, Membrane fouling in desalination

and its mitigation strategies, Desalination 425 (2018) 130–155.
[9] Hadeel Subhi Abid, Daniel James Johnson, Raed Hashaikeh, Nidal Hilal, A review of efforts to reduce membrane fouling by control of feed spacer characteristics, Desalination 420 (2017) 384–402.
[10] Shanxue Jiang, Yuening Li, Bradley P. Ladewig, A review of reverse osmosis membrane fouling and control strategies, Sci. Total Environ. 595 (2017) 567–583.
[11] Xu Su Wende Li, Alan Palazzolo, Shehab Ahmed, Erwin Thomas, Reverse osmosis membrane, seawater desalination with vibration assisted reduced inorganic fouling, Desalination 417 (2017) 102–114.
[12] Haigang Li, Huanjin Xia, Yingxin Mei, Modeling organic fouling of reverse osmosis membrane: from adsorption to fouling layer formation, Desalination 386 (2016) 25–31.
[13] Aleix Benito, Gerard Garcia, Rafael Gonzalez-Olmos, Fouling reduction by UV-based pretreatment in hollow fiber ultrafiltration membranes for urban wastewater reuse, J. Membr. Sci. 536 (2017) 141–147.
[14] Rafael Kuwertz, Carina Kirstein, Thomas Turek, Ulrich Kunz, Influence of acid pretreatment on ionic conductivity of Nafion® membranes, J. Membr. Sci. 500 (2016) 225–235.
[15] Lisa Henthorne, Buddy Boysen, State-of-the-art of reverse osmosis desalination pretreatment, Desalination 356 (2015) 129–139.
[16] Kamel Fethi, Chheibi Habib, Performances de la Station de Dessalement de Gabes (22,500 m^3/j) après cinq ans de fonctionnement, Desalination 136 (2001) 263–272.
[17] Mohamed Belkacem, Saida Bekhti, Kenza Bensadok, Groundwater treatment by reverse osmosis, Desalination 206 (2007) 100–106.
[18] Hamza Elfil, Henri Roques, Prediction of the limit of the metastable zone in the "$CaCO_3$ – CO_2 – H2O" system, AICHE J. 50 (8) (2004) 1908–1916.
[19] Shengtong Sun, Denis Gebauer, Helmut Cölfen, A solvothermal method for synthesizing monolayer protected amorphous calcium carbonate clusters, Chem. Commun. 52 (2016) 7036–7038.
[20] Matthias Kellermeier, Andreas Picker, Andreas Kempter, Helmut Cölfen, Denis Gebauer, A straightforward a treatment of activity in aqueous $CaCO_3$ solutions and the consequences for nucleation theory, Adv. Mater. 26 (55) (2014) 752–757.
[21] Matthias Kellermeier, Paolo Raiteri, John K. Berg, Andreas Kempter, Julian D. Gale, Denis Gebauer, Entropy drives calcium carbonate ion association, ChemPhysChem 17 (21) (2016) 3535–3541.
[22] Kenneth S. Pitzer, Guillermo Mayorga, Thermodynamics of electrolyte. III. Activity and osmotic coefficients for 2-2 electrolytes, J. Solut. Chem. 3 (1974) 539–546.
[23] Yosra Zarga, H. Ben Boubaker, Nordine Ghaffour, Hamza Elfil, Study of calcium carbonate and sulfate co-precipitation, Chem. Eng. Sci. 96 (2013) 33–41.
[24] Hamza Elfil, Ahmed Hannachi, Reconsidering water scaling tendency assessment, AICHE J. 52 (2006) 3583–3591.
[25] Khaled Touati, Mehdi Hila, Kalthoum Makhlouf, Hamza Elfil, Study of fouling in two-stage reverse osmosis desalination unit operating without an inlet pH adjustment: diagnosis and implications, Water Sci. Technol. Water Supply 17 (6) (2017) 1682–1693.